environments

MDPI

Article

Preliminary Insights into the Inflammatory and Oxidative Effects of Galaxolide (HHCB) in the Medicinal Leech *Hirudo verbana*

Alberto Rihan [1], Gaia Marcolli [1], Marina Borgese [2], Laura Pulze [1], Annalisa Grimaldi [1], Nicolò Baranzini [1,*] and Stefano Tasselli [3,*]

[1] Department of Biotechnology and Life Sciences, University of Insubria, 21100 Varese, Italy; arihan@studenti.uninsubria.it (A.R.); gmarcolli@uninsubria.it (G.M.); laura.pulze@uninsubria.it (L.P.); annalisa.grimaldi@uninsubria.it (A.G.)
[2] Department of Medical Innovation and Technology, University of Insubria, 21100 Varese, Italy; marina.borgese@uninsubria.it
[3] National Research Council-Water Research Institute (CNR-IRSA), Via del Mulino 19, 20861 Brugherio, Italy
* Correspondence: nicolo.baranzini@uninsubria.it (N.B.); stefanotasselli@cnr.it (S.T.)

Abstract

Galaxolide (HHCB), a synthetic polycyclic musk widely used as a fragrance ingredient in numerous personal care and household products, has raised increasing environmental concern due to its persistence, bioaccumulation potential, and widespread occurrence in aquatic environments. In this context, the need to establish a concrete ecotoxicological risk profile, defining both the toxicity levels and the mechanisms of action, is fundamental. For this reason, in the current study, we selected the freshwater leech *Hirudo verbana* as a suitable in vivo model to assess the HHCB ability in inducing inflammatory response and oxidative stress. By means of morphological, immunofluorescence, and molecular analyses, HHCB was shown not only to affect the leech innate immune response by modulating angiogenesis and macrophage-like cells recruitment, but also to promote the expression of enzymes involved in the antioxidant response, such as superoxide dismutase (SOD), glutathione S-transferase (GST) and catalase (CAT). Overall, these findings indicate that HHCB could induce significant physiological alterations, with sub-lethal concentrations able to affect immune homeostasis. Furthermore, this study supports the use of alternative invertebrate models to better understand the possible harmful effects of emerging contaminants.

Keywords: Galaxolide; inflammation; medicinal leech; oxidative stress; immune response

Check for updates

Academic Editor: Daniele Fattorini

Received: 11 April 2026
Revised: 13 May 2026
Accepted: 16 May 2026
Published: 20 May 2026

Copyright: © 2026 by the authors. Licensee MDPI, Basel, Switzerland. This article is an open access article distributed under the terms and conditions of the Creative Commons Attribution (CC BY) license.

1. Introduction

The term emerging micropollutants (EMPs) refers to a broad and heterogeneous group of chemicals that are not yet fully subject to regulation nor routinely monitored by conventional protocols [1–6]. These substances are typically present at extremely low concentrations, often difficult to quantify, in the order of micrograms per liter (μg L^{-1}) or even nanograms per liter (ng L^{-1}) [7–10]. They include pharmaceuticals, personal care products, novel pesticides, per- and polyfluoroalkyl substances (PFAS), flame retardants, as well as micro- and nanoplastics. Being characterized by both high persistence and bioaccumulation potential, their environmental fate, behavior, and ecotoxicological effects remain largely unexplored, with increasing evidence that suggests possible adverse effects already at very low concentrations [11–14]. In addition, many EMPs also undergo degradation to metabolites or secondary products that often result in more biologically active or even more toxic than the parental compounds [15–18].

The environmental release of EMPs occurs through different sources, often diffuse and difficult to control. Most of them originate from urban discharges, including pharmaceuticals and personal care products, which reach the wastewater treatment plants (WWTPs) through urban sewage systems [19–26]. Among industrial activities, sectors such as textile manufacturing, electroplating, and chemical production are the major contributors to EMP emission, while intensive agriculture represents another crucial source, particularly through the runoff of pesticides and fertilizers. Indeed, wastewater treatment plants (WWTPs) are not specifically designed to remove these microcontaminants, and therefore, conventional treatment technologies are generally inefficient in eliminating them; as a result, due to their continuous input, these compounds often pass through the treatment processes largely unaltered. Thus, their environmental fate results extremely heterogeneous, as it often depends on their physicochemical properties and on the characteristics of the medium in which they are distributed [27].

In this context, among the various classes of EMPs, synthetic fragrances constitute a category of emerging chemicals subject to considerable attention. These molecules are commonly classified as Personal Care Products (PCPs), a group of products intended for personal hygiene and household cleaning, and are present in a wide range of items, including perfumes, lotions, hair and skin care formulations, detergents, fabric softeners, and indoor air fresheners [28–31]. Given their widespread use, increasing evidence has highlighted their occurrence predominantly in the aquatic ecosystems, suggesting a potential risk of bioaccumulation in organisms inhabiting these environments [32–36]. Currently, these artificial fragrances have been classified into three distinct categories, based on their chemical structure: nitromusks, macrocyclic musks, and the most used polycyclic musks [37]. The latter comprises semi-volatile and hydrophobic molecules characterized by non-polar functional groups. In aquatic environments, these fragrances tend to associate with sediments or suspended particulate organic matter, or to accumulate within the biota [38–42]. For these reasons, the attention of the scientific community has grown significantly, due to their bioaccumulation and biomagnification potential, together with possible harmful effects [43,44].

In particular, Galaxolide (HHCB) still occupies about 95% and 90% of the European and US polycyclic musk category markets, respectively, representing one of the most diffused, Liu et al., 2023 [45,46]. This synthetic musk is widely used as a fragrance ingredient in a broad range of consumer products. It was developed as an alternative to natural musks and earlier nitro musks, and it is valued for its pleasant and persistent scent [47]. In addition to aquatic environments, HHCB has also been detected in human tissues, including blood, adipose tissue, and breast milk [48]. Indeed, this molecule enters the human body through multiple exposure routes, including dermal absorption, inhalation, and ingestion. Due to its lipophilic nature, it readily crosses biological membranes and tends to accumulate in lipid-rich tissues, explaining its detection in these specific human matrices [48–53]. For these reasons, HHCB has increasingly attracted regulatory attention in recent years. In the European Union, it is regulated as a fragrance ingredient under the EU Cosmetics Regulation (EC) No. 1223/2009, and under the CLP Regulation (EC) No. 1272/2008, where it is currently classified as a possible toxicant to aquatic environments. Currently, HHCB is under re-evaluation by the European Chemical Agency (ECHA) as a Persistent, Bioaccumulative and Toxic (PBT) and Endocrine Disrupting (ED) substance, following a submission by the Agence nationale de sécurité sanitaire (ANSES) [54]. In Italy, high levels of HHCB have already been detected in aquatic environments with concentrations often exceeding 100 ng L^{-1}, representing a potential concern also for our ecosystems [55,56]. The widespread occurrence of this compound, together with its persistence and high bioaccumulation potential, highlights concern about its potential toxicity in aquatic ecosystems.

Consequently, a comprehensive assessment of the ecological effects associated with HHCB exposure becomes essential to better understand the potential impacts and to support informed environmental management and regulatory decisions [55,56]. The widespread occurrence of this compound, together with its persistence and high bioaccumulation potential, highlights concern about its potential toxicity in aquatic ecosystems. Consequently, a comprehensive assessment of the ecological effects associated with HHCB exposure becomes essential to better understand the potential impacts and to support informed environmental management and regulatory decisions.

To date, despite the literature data on HHCB bioaccumulation potential, endocrine-disrupting activity, and oxidative stress-mediated toxicity are present in several organisms, the current knowledge remains largely confined to classical toxicological endpoints and standard test species [57–61]. In particular, outside conventional toxicity assays, limited information is available on the sublethal effects of HHCB on immune responses, inflammatory processes, and metabolism, which represent critical and highly conserved physiological targets of environmental contaminants. For these reasons, the present study aims to investigate the possible adverse effects induced by HHCB both at the molecular and cellular levels, with particular focus on the modulation of the innate immune response, using the medicinal leech *Hirudo verbana* as an in vivo model organism. The choice of this freshwater invertebrate is not arbitrary but arises from a strategic convergence between its ecological relevance and the well-known anatomical and physiological characteristics. Indeed, leeches represent a promising model for freshwater ecotoxicological investigations due to their biological sensitivity, ecological relevance, and methodological advantages. Medicinal leeches are highly sensitive to environmental contaminants, including heavy metals and emerging pollutants, exhibiting measurable behavioral, physiological, immune, and oxidative stress responses even at sublethal concentrations [62–64]. From an ecological perspective, *H. verbana* inhabits both the water column and benthic substrates, allowing for the assessment of the exposure to contaminants dissolved both in water and accumulated within sediments, thus representing different freshwater environmental compartments. Moreover, these organisms are easy to maintain under laboratory conditions and tolerate handling and prolonged fasting periods, facilitating both acute and chronic exposure studies under controlled and reproducible experimental conditions. For these reasons, this species represents a well-established experimental model for investigating the potential HHCB toxic effects, providing a sensitive and integrative framework to explore biological responses that are poorly addressed in more traditional studies.

2. Materials and Methods

2.1. Experimental Exposure

- Leeches of the species *Hirudo verbana* (Annelida, Hirudinea), obtained from our breeding facility (Italian Leech Farm ILFARM, Varese, Italy), were kept in sealed jars at 20 °C in slightly salted water (NaCl 1.5 g L^{-1}). Twenty-seven leeches were randomly assigned to three experimental groups (9 individuals per group), each consisting of three independent replicates with three animals each, and exposed to the following treatments: Group 1: untreated leeches (N.T., n = 9), used as control.
- Group 2: leeches (n = 9) exposed to acetone (C_3H_6O) (0.001% v/v), named as SOLV.
- Group 3: leeches (n = 9) exposed to 10 μg L^{-1} of HHCB.

The HHCB stock solution (1 mg mL^{-1}) was diluted to a final concentration of 10 mg L^{-1} in acetone. In each replicate, 200 μL of HHCB 10 mg L^{-1} was added to 200 mL of lightly salted water (NaCl 1.5 g L^{-1}) to reach a final concentration of 10 μg L^{-1}. Test concentration was intentionally set one order of magnitude higher than those previously measured in Italian WWTP effluents [65] ref in order to account for the intrinsic variabil-

ity and uncertainty associated with environmental exposure scenarios. Concentrations detected in treated effluents may fluctuate substantially over time due to variations in influent composition, treatment efficiency, hydraulic conditions, and episodic discharge events. Therefore, the use of an exposure concentration exceeding the average measured environmental level represents a conservative and ecologically relevant approach. Samples were stored in a dark room to avoid possible photodegradation of the molecule. After 24 h, exposure solutions were completely renewed since a previous experiment to assess HHCB stability in the same water showed a decrease of 22% in concentration in 24 h, and animals were transferred into new jars for a further 24 h. After 48 h from the beginning of the experiment, animals were sacrificed after 5 min of immersion in a 10% ethanol solution, used as an anesthetic.

Chemical analyses were carried out to verify the HHCB concentration in water at t_0, 24 h, and 48 h by analyzing pooled replicates from each experimental condition, as well as in animal tissues at the end of the exposure using pooled organisms from the same group. Analyses were performed by GC-MS/MS with a Trace 1310 gas chromatograph coupled to a TSQ 8000 Evo Triple Quadrupole mass spectrometer (ThermoFisher Scientific, Waltham, MA, USA), according to the methodology described in [20].

The in vivo experiments were performed using medicinal leeches belonging to the species *Hirudo verbana*, which are not included among the species protected under Directive 2010/63/EU regulating the use of animals for scientific purposes, nor under the Italian Legislative Decree no. 26 of 4 March 2014 implementing the same directive. Nevertheless, the experimental protocol was approved by the Animal Welfare Body (OPBA) of the University of Insubria.

2.2. Embedding of Tissues in Epoxy Resin for Light and Transmission Electron Microscopy (TEM) Analyses

Leech tissues were carefully dissected and fixed for 2 h at room temperature in 4% glutaraldehyde diluted in 0.1 M cacodylate buffer (pH 7.4). After several washes in the same buffer, samples were post-fixed for 1 h in the dark with 2% osmium tetroxide (OsO_4). Specimens were then rinsed again in 0.1 M cacodylate buffer and dehydrated through an ascending ethanol series (30%, 50%, 70%, 90%, 96%, and absolute ethanol). Subsequently, tissues were incubated for 1 h in a 1:1 propylene oxide/resin solution and finally embedded in Epon-Araldite 812 epoxy resin (Sigma-Aldrich, Milan, Italy).

Semithin sections (750 nm) intended for light microscopy were obtained using an RMC Power Tome XL ultramicrotome (Boeckeler Instruments, Tucson, AZ, USA), mounted on glass slides, and stained with crystal violet (1 g/100 mL distilled water) and basic fuchsin (0.13 g/100 mL distilled water). Observations were performed with a Nikon Eclipse microscope, and images were captured using a DS-5M-L1 digital camera system (Nikon, Tokyo, Japan). Ultrathin sections (70 nm) from the same specimens were collected on 300-mesh copper grids, contrasted with uranyl acetate and lead citrate, and examined using a JEOL1400Plus transmission electron microscope at the Centro di Ricerca e Trasferimento Tecnologico (CRIETT), University of Insubria (instrument code MIC01). Micrographs were acquired using a MORADA digital camera system (Olympus, Tokyo, Japan).

2.3. Embedding Tissue in OCT for Cryosections and Immunofluorescence Assays on Cryosections

Collected leech samples were immediately embedded in OCT (Optimal Cutting Temperature) compound (Polyfreeze, TebuBio, Le Perray-en-Yvelines, France), rapidly frozen in liquid nitrogen, and stored at −80 °C until processing. Cryosections (7 µm thick) were obtained using a Leica CM1850 cryostat, mounted on gelatin-coated slides, and preserved at −20 °C. Prior to staining, sections were rehydrated for 10 min in PBS (138 mM NaCl, 2.7 mM KCl, 4.3 mM Na_2HPO_4; pH 7.4) and then incubated for 30 min in a blocking

solution composed of 2% bovine serum albumin (BSA) and 0.1% Tween in PBS. The same BSA-based solution was used to dilute both primary and secondary antibodies.

Samples were incubated for 1 h at room temperature with the following rabbit polyclonal primary antibodies: anti-CD31 (Santa Cruz Biotechnology, Dallas, TX, USA; diluted 1:200) and anti-Iba1 (Proteintech, Rosemont, IL, USA; diluted 1:150). After extensive PBS washes, tissues were incubated for 45 min with FITC-conjugated secondary antibodies (ThermoFisher Scientific, MA, USA; diluted 1:250). Nuclear counterstaining was performed using 4′,6-diamidino-2-phenylindole (DAPI; 0.1 mg/mL in PBS) for 5 min, after which slides were mounted with PBS/Glycerol Cityfluor mounting medium (Cityfluor Ltd., Hatfield, UK). Negative controls were prepared by omitting the primary antibodies.

Fluorescence signals were analyzed using a Nikon Digital Sight DS-SM fluorescence microscope (Tokyo, Japan). FITC and DAPI fluorescence were visualized using excitation/emission filters of 490/525 nm and 340/488 nm, respectively. Final image acquisition, processing, and merging were carried out with Adobe Photoshop (Adobe Systems, Inc., San Jose, CA, USA).

2.4. RNA Extraction and Quantitative PCR (qPCR)

Leech tissues were immediately frozen in liquid nitrogen and mechanically ground using a mortar. The resulting powder was resuspended in 1 mL of TRIzol reagent (Life Technologies, Carlsbad, CA, USA), centrifuged at 12,000 rpm for 10 min, and incubated at room temperature for 5 min. Subsequently, 200 µL of chloroform was added to each sample, followed by centrifugation at 13,000 rpm for 15 min at 4 °C. After phase separation, 500 µL of the aqueous phase was transferred into a fresh tube and mixed with an equal volume of isopropanol. Samples were then incubated for 10 min at room temperature and centrifuged again at 13,000 rpm for 10 min. The resulting RNA pellets were washed with 75% ethanol and finally resuspended in 30 µL of DEPC-treated water. RNA quantity was determined spectrophotometrically, while RNA integrity was verified on a 1% agarose gel. For cDNA synthesis, 2 µL of RNA was reverse transcribed using M-MLV reverse transcriptase (Life Technologies, Carlsbad, CA, USA). Quantitative PCR reactions were performed in triplicate using the Bio-Rad CFX Connect Real-Time PCR Detection System (Bio-Rad Laboratories, Hercules, CA, USA). After an initial denaturation step, amplification was carried out for 39 cycles under the following conditions: 95 °C for 10 s, 60 °C for 5 s, and 72 °C for 10 s. Relative transcript levels were determined according to the $2-\Delta\Delta Ct$ method, using 18S as the housekeeping gene. Primer sequences employed for qPCR analyses are listed in Table 1:

Table 1. List of primers used for qPCR analyses.

Target Genes	Primers	Product Size (bp)
*Hm*AIF-1	Fw: 5′-GACCTCAAAGACAAGCAGGG-3′	229
	Rev: 5′-GGCCAATCTTCTCCAGCATC-3′	
GST	Fw: 5′-AGACACATCGCCAGGACTAA-3′	127
	Rev: 5′-ACGGATACACGACTCCAACT-3′	
SOD	Fw: 5′-ATCCTCTTGAACCCACCACA-3′	95
	Rev: 5′-ATCTGGACGCACATTCTTGT-3′	
CAT	Fw: 5′-ACCGCCTGGGAACAAATTAC-3′	117
	Rev: 5′-AATTAGGAGCATCGCCTTGG-3′	
VEGF-A	Fw: 5′-GATGTTCAGGCTGTTGCTA-3′	142
	Rev: 5′- TGTTCCTCAATGTCCACTTC-3′	

2.5. Western Blot Analyses

Similar to the procedure adopted for qPCR analyses, leech tissues were rapidly frozen in liquid nitrogen and mechanically homogenized. The resulting tissue powder was resuspended in RIPA buffer (150 mM NaCl, 1% NP-40, 0.5% sodium deoxycholate, 0.1% SDS, 50 mM Tris-HCl, pH 8.0) using 10 µL of buffer per mg of tissue, supplemented with a protease inhibitor cocktail (Sigma-Aldrich, Milan, Italy). Cellular debris was removed by centrifugation at 15,000 rpm for 10 min at 4 °C using a refrigerated Eppendorf Minispin microcentrifuge (Eppendorf, Hamburg, Germany). Protein concentration was determined using the Coomassie Brilliant Blue G-250 assay (Pierce, Rockford, IL, USA), with BSA employed as the standard protein reference. Aliquots containing 40 µg of total proteins were denatured at 95 °C for 5 min and separated by SDS-PAGE on 12% acrylamide gels. Proteins were then transferred onto nitrocellulose membranes using a gel transfer system operated at 350 mA for 2 h. Membranes were blocked for 2 h at room temperature in 5% nonfat dry milk prepared in Tris-buffered saline (TBS; 20 mM Tris-HCl, 500 mM NaCl, pH 7.5) and subsequently incubated for 90 min with the following primary antibodies: rabbit anti-VEGF-A (ThermoFisher Scientific, MA, USA; 1:500 dilution in 5% milk) and rabbit anti-*Hm*AIF-1 (1:4000 dilution in 5% milk; kindly provided by Professor Vizioli, University of Lille, France). Following three washes in TBS containing 0.1% Tween-20, membranes were incubated with horseradish peroxidase-conjugated anti-rabbit IgG secondary antibody (Jackson ImmunoResearch Laboratories, West Grove, PA, USA) diluted 1:5000. Immunoreactive bands were detected using LiteAblot PLUS Enhanced Chemiluminescent Substrate (EuroClone, Pero, Italy). Band intensity was quantified using ImageJ (National Institutes of Health, Bethesda, MD, USA, version 1.53e), and values were normalized to the housekeeping protein glyceraldehyde-3-phosphate dehydrogenase (GAPDH), detected with a rabbit polyclonal anti-GAPDH antibody (Proteintech, Rosemont, IL, USA) diluted 1:5000.

2.6. Acid Phosphatase Assay (ACP)

Cryosections prepared as previously described were rehydrated in PBS for 10 min and subsequently incubated for 5 min in 0.1 M sodium acetate–acetic acid buffer. Sections were then treated with a reaction mixture containing 0.1 M sodium acetate–acetic acid buffer, 0.01% naphthol phosphate, 2% N,N-dimethylformamide, 0.06% Fast Red, and 0.5 nM $MnCl_2$, and incubated for 90 min at 37 °C. Following repeated washes in PBS, slides were mounted using Cityfluor mounting medium (Cityfluor Ltd., Hatfield, UK) and analyzed under a light microscope, as previously described.

2.7. Paraffin Embedding and Histochemical Analysis of Mucus Cells by PAS Staining

Leech tissues were fixed in 4% paraformaldehyde for 1 h. After five washes of 5 min each in 1× PBS, samples were dehydrated through an ascending ethanol series (30%, 50%, 70%, 90%, 96%, and 100%). Specimens were then incubated overnight in a 1:1 paraffin/xylol solution and finally embedded in paraffin. Sections (0.7 µm thick) were obtained using a Jung 2045 paraffin microtome (Leica, Vienna, Austria) and processed for Periodic Acid–Schiff (PAS) histochemical staining according to the manufacturer's instructions (PAS kit, Bio Optica, Milan, Italy). Samples were subsequently observed under a light microscope, and images were acquired as previously described.

2.8. Statistical Analyses

All experiments were carried out in triplicate, and graph values are presented as means. Statistical analyses were performed using GraphPad Prism version 8 (GraphPad Software, La Jolla, CA, USA). Significant differences among experimental groups were

evaluated by one-way ANOVA, followed by Tukey's post hoc test. Differences were considered statistically significant at $p < 0.05$. For the quantification of blood vessels and ACP^+ macrophages, ten different slides per experimental group were analyzed, considering random fields of 45,000 μm^2 for each slide, using ImageJ. Data in graphs are expressed as mean values ± standard deviation (SD), while asterisks indicate statistically significant differences between control and HHCB-treated samples.

3. Results

3.1. Characterization of the Angiogenic Processes

The potential HHCB ability to induce leech inflammatory response has been first evaluated by assessing the activation of angiogenic processes (Figure 1). In these aquatic organisms, the formation of new blood vessels represents a key functional process during the initial phase of inflammation. Light microscopy morphological analyses revealed that in control samples (Figure 1a,b) tissues appeared largely avascular, with only a few small physiological vessels confined underneath the epithelium and surrounding muscle fibers. Contrariwise, an improved vascularization was clearly detectable in HHCB-treated samples (Figure 1c), where the number of neo-formed blood vessels was higher, as also confirmed by the total vessels count shown in the graph (Figure 1g). The pro-angiogenic effects of HHCB were also highlighted by assessing the botryoidal tissue organization (Figure 1d–f). Indeed, in control samples, botryoidal cells were characterized by a grape-like, tightly packed morphology (Figure 1d,e), typical of an inactive state. Instead, the same cells showed a more distal distribution and a less compact organization when leeches were exposed to this synthetic compound (Figure 1f). Moreover, this spacing allowed the observation of newly formed vascular lumens in the central region.

3.2. Immunofluorescent and Molecular Analyses

Previous morphological observations were further supported by immunofluorescence analysis using an anti-CD31 antibody, a specific marker of endothelial cells (Figure 2a–d). In untreated and solvent-treated samples, a low fluorescent signal was detectable underneath the epithelium and in the close connective tissue (Figure 2a,b), while after the HHCB exposure, the number of CD31-positive cells increased (Figure 2c), as also confirmed by the quantification of the total fluorescent area shown in the graph (Figure 2d). In addition, both qPCR and Western blot assays revealed a significant increase in the expression of VEGF-A in HHCB-treated leeches compared to controls (Figure 2e,f). These growth factors usually stimulate endothelial cell proliferation, migration, and survival, thereby promoting angiogenesis and increasing vascular permeability.

3.3. Recruitment of Macrophage-like Cells Induced by HHCB

During inflammation, the formation of new blood vessels in leeches is normally strictly correlated with the recruitment of innate immune cells, in particular macrophage-like cells. For this reason, the possible HHCB ability in recruiting this specific cell population was investigated by means of light and TEM, together with acid phosphatase (ACP) histoenzymatic assay (Figure 3). In untreated or solvent-treated leeches, only a few macrophage-like cells were clearly detectable in the extracellular matrix around muscle fibers (Figure 3a). Conversely, animals exposed to HHCB (Figure 3b) showed a significant increase in the number of these immune cells. Ultrastructural analyses at TEM confirmed this evidence (Figure 3c), in which several activated macrophages, characterized by the presence of cytoplasmatic pseudopodia, have been observed. Given that activated macrophages are characterized by an intense phagocytic activity, ACP histoenzymatic analyses have been performed (Figure 3d–f). In tissues of control and solvent-exposed animals, only a few ACP-

positive cells were visible (Figure 3d,e), while after HHCB administration (Figure 3f), their number was significantly enhanced. This data was also confirmed by the total ACP-positive cells count, reported in the related graph (Figure 3g).

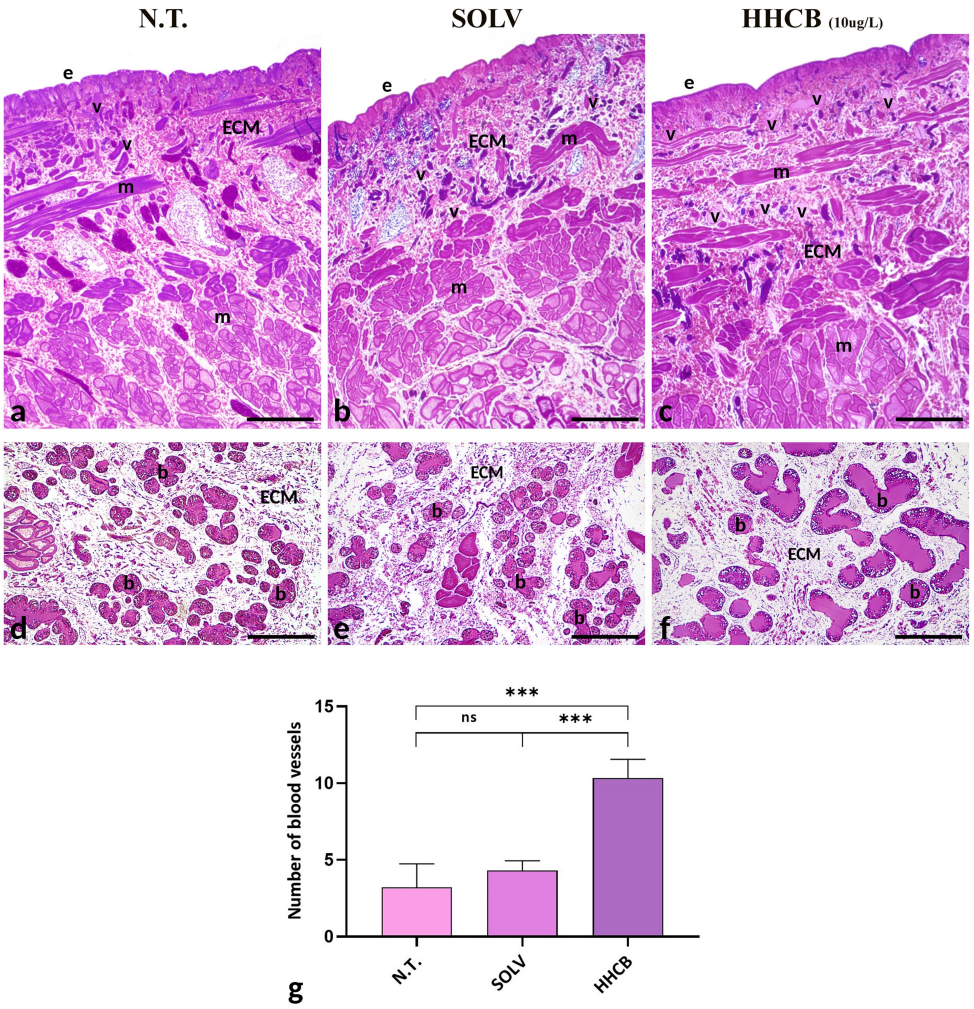

Figure 1. Evaluation of the leech angiogenic process activation. In both untreated (**a**) and solvent-treated (**b**) samples, tissues appear predominantly avascular, with only a few blood vessels (v) present close to the epithelium (e) and to the muscle fibers (m) localized in the extracellular matrix (ECM) below. In contrast, a significant increase in the number of new blood vessels is visible after HHCB exposure (**c**). This data is also confirmed by the evaluation of the botryoidal tissue (**d**–**f**), in which the botryoidal cells' morphology significantly changes (b) after HHCB administration. The graph shows the total vessel count based on the light microscopy images (**g**). In the graph, $p < 0.05$ is considered statistically significative (*** $p < 0.001$). Bars in (**a**–**c**): 100 µm; bars in (**d**–**f**): 50 µm.

3.4. Expression of HmAIF-1 Pro-Inflammatory Cytokine

To confirm the activation of leech macrophage-like cells following HHCB exposure, the expression of *Hm*AIF-1, a fundamental pro-inflammatory factor specifically produced by this cell population, has been assessed by means of immunofluorescent and molecular analyses (Figure 4). Immunolabelling assays, performed using an anti-Iba1 antibody (recognizing the leech *Hm*AIF-1 homolog), revealed that in untreated (Figure 4a) or solvent-treated samples (Figure 4b), a lower *Hm*AIF-1 signal was present, with few resident positive cells localized close to the epithelium and surrounding muscle fibers. On the contrary, in animals exposed to HHCB, the number of *Hm*AIF-1$^+$ cells was higher (Figure 4c), as also confirmed by the analyses of the total fluoresce area (Figure 4d). In addition, molecular analyses, conducted by means of both qPCR and Western blot experiments (Figure 4e,f),

supported this evidence, showing a significant increase in the *Hm*AIF-1 expression levels in HHCB-treated leeches.

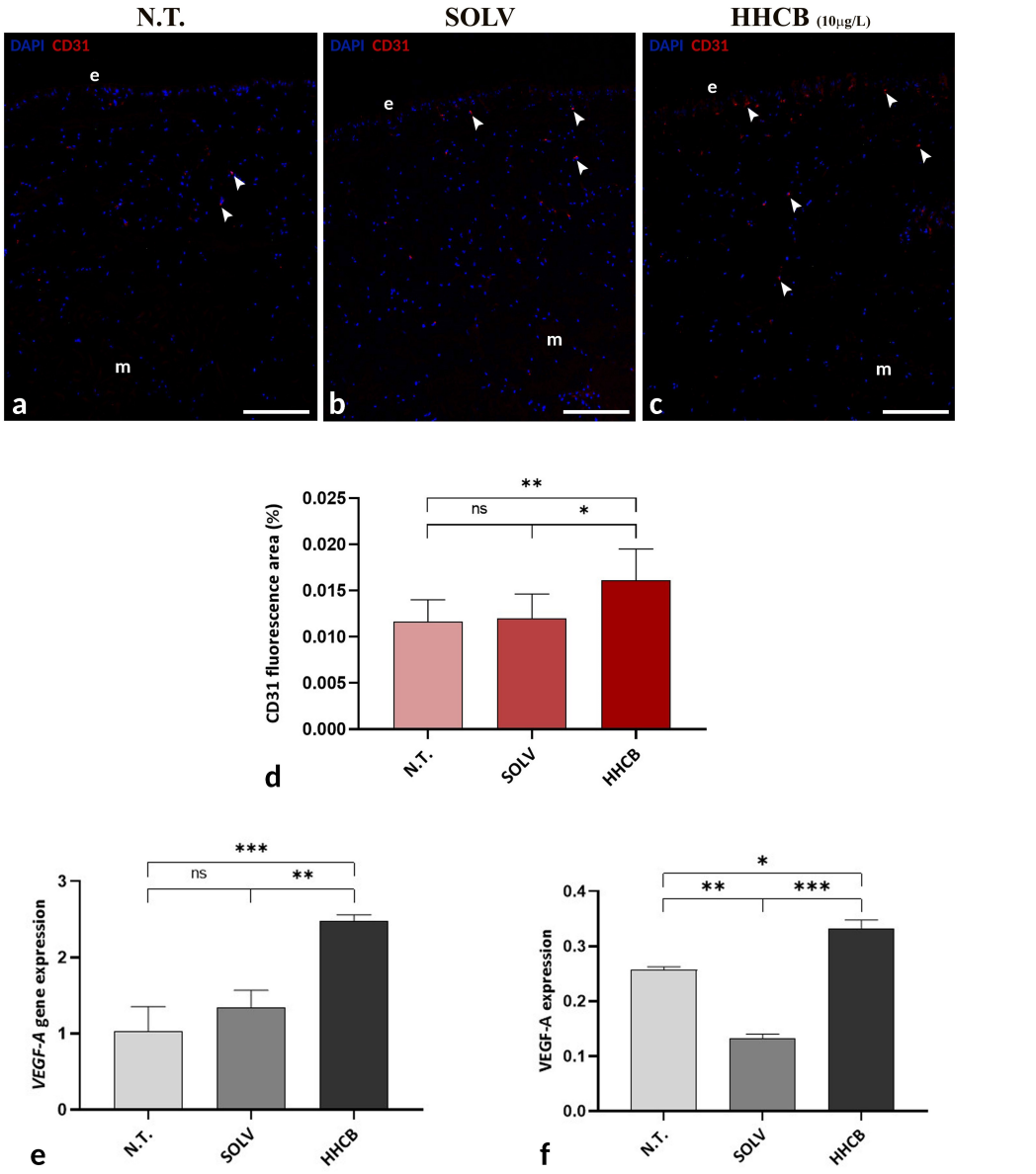

Figure 2. Immunolocalization and molecular analyses to confirm the angiogenic stimulation. Immunolabelling experiments using anti-CD31 antibody (**a**–**c**) reveal that numerous CD31$^+$ cells (white arrowheads) are visible near the epithelium (e) in HHCB-treated leeches, compared to controls, as also confirmed by the analyses of the total fluorescent signal (**d**). Moreover, qPCR (**e**) and Western blot (**f**) analyses suggest that the expression of VEGF-A significantly increased after HHCB exposure, compared to controls. m: muscle fibers. In panels (**a**–**c**), red indicates CD31 immunoreactivity, while blue indicates DAPI-stained nuclei. In the graphs, $p < 0.05$ is considered statistically significative (* $p < 0.05$, ** $p < 0.01$, *** $p < 0.001$). Bars in (**a**–**c**): 100 μm.

3.5. Assessment of the Oxidative Stress Enzymes Gene Expression

Given that the presence of pollutants usually promotes antioxidative defense in leeches, the possible HHCB involvement in stimulating oxidative stress was also evaluated. In detail, the expression of specific conserved enzymes, normally triggered during the oxidative response, has been evaluated by qPCR analyses (Figure 5).

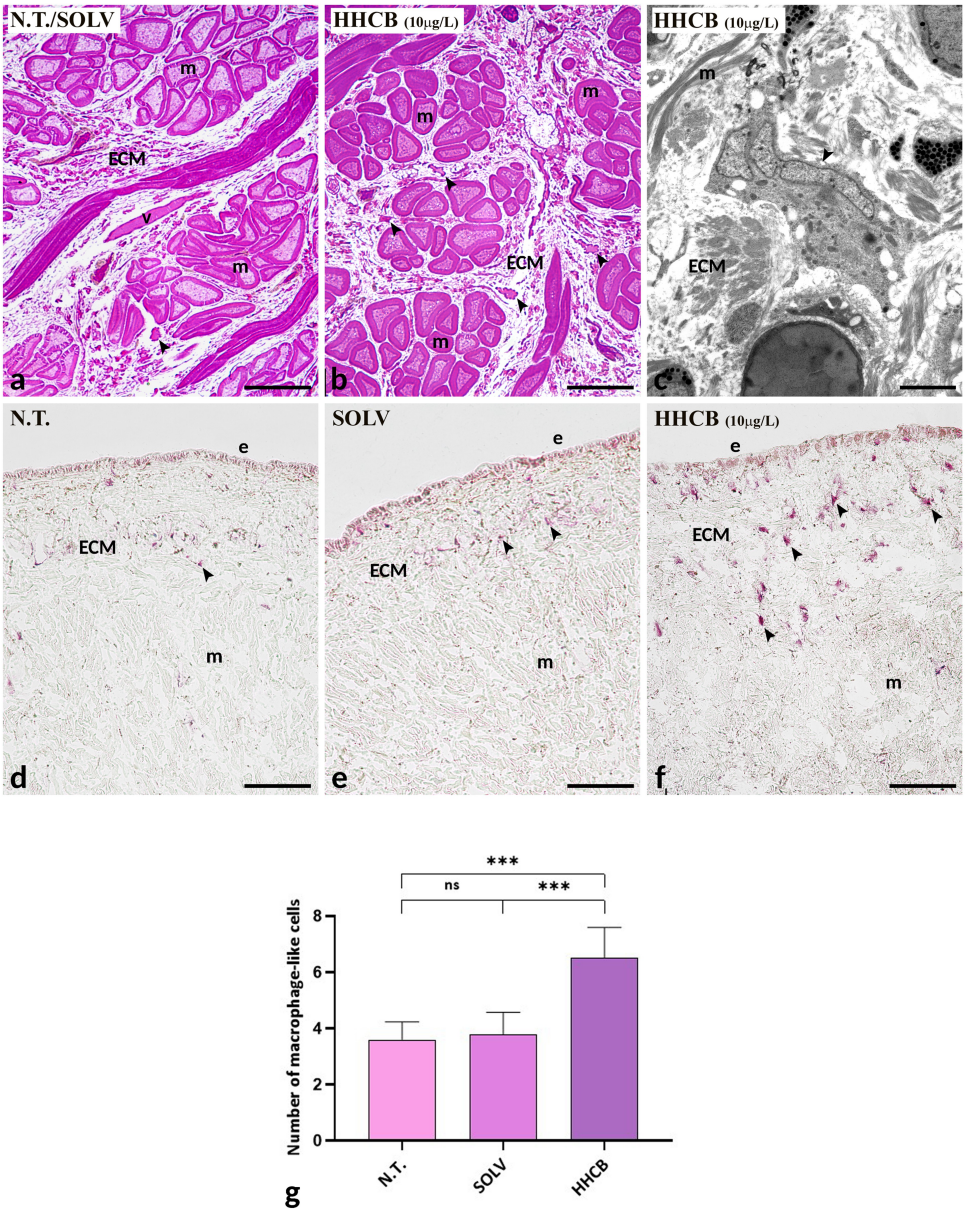

Figure 3. Evaluation of macrophage-like cells recruitment. Few resident macrophages (black arrowheads) are located close to the epithelium (e), among muscle fibers (m) and in the extracellular matrix (ECM) in control samples (**a**), while a significant increase in these immune cells is observable in HHCB-treated samples (**b**), as confirmed by ultrastructural analyses at TEM (**c**). Acid phosphatase assay shows an increase in ACP^+ phagocytic cells, especially in HHCB-treated samples, compared to controls (**d**–**f**). The graph shows the mean number of ACP^+ cells in each sample (**g**). $p < 0.05$ is considered statistically significative (*** $p < 0.001$). Bars in (**a**,**b**): 20 µm; bar in (**c**): 2 µm; bars in (**d**–**f**): 100 µm.

The obtained results demonstrated a marked upregulation in the transcripts encoding superoxide dismutase (*SOD*), glutathione S-transferase (*GST*), and catalase (*CAT*) genes (Figure 5a–c). The simultaneous induction of these enzymes provided direct molecular evidence of an elevated oxidative challenge.

3.6. Evaluation of Leech Secretory Cells in Response to HHCB

In leeches, activation of mucus cells is typically observed as a protective response to environmental pollutants and oxidative stress. Their morphological response was therefore

assessed using PAS histochemical staining (Schiff's Periodic Acid) staining, which allows them to differentiate Type 1 and Type 2 mucus cells in leech tissues.

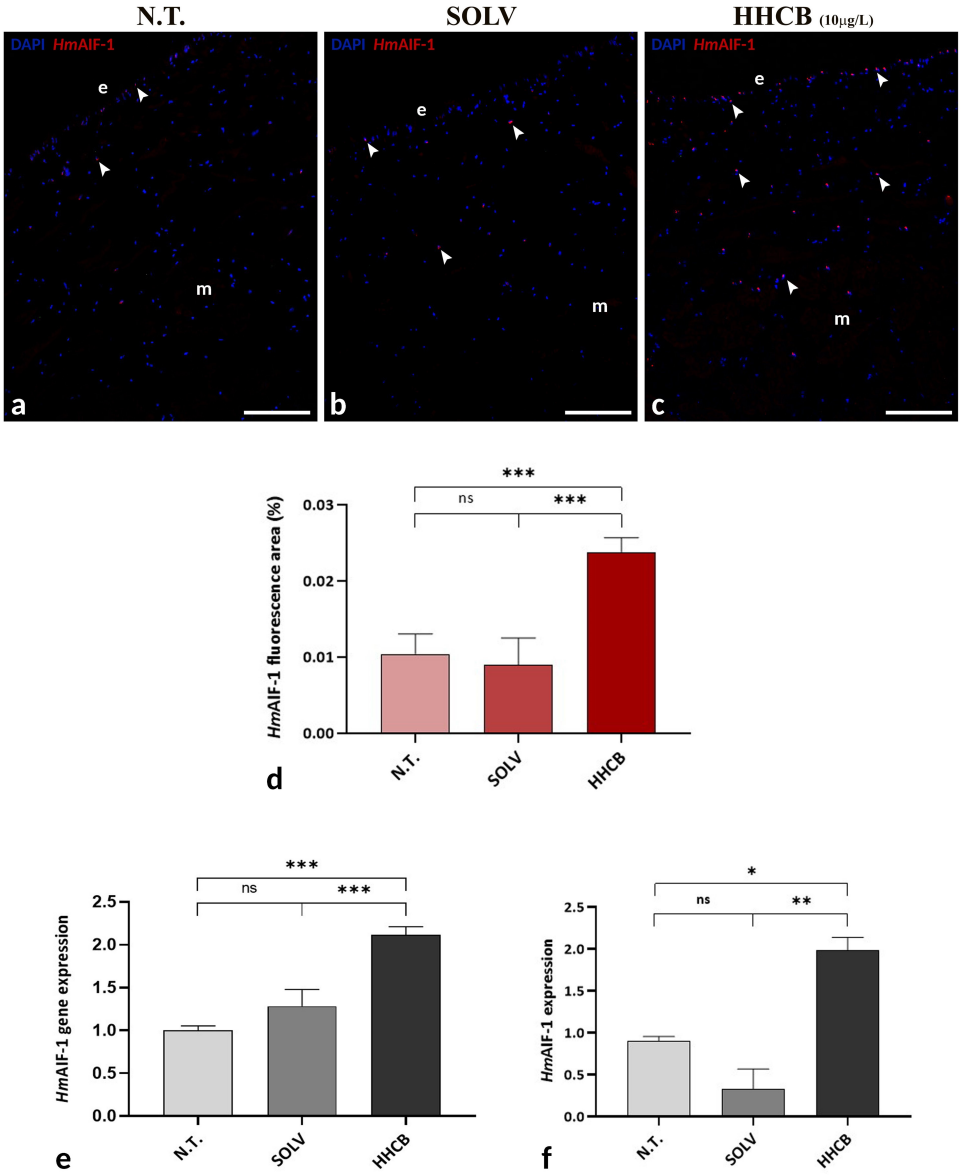

Figure 4. Evaluation of the expression of *Hm*AIF-1, a pro-inflammatory cytokine, specifically expressed by leech macrophages. Immunofluorescence analyses using anti-Iba1 antibody (**a**–**c**) show a low number of positive cells in both untreated and solvent-treated leeches (**a**,**b**), whereas an increase in *Hm*AIF-1 positive cells (white arrowheads), situated in the epithelium (e) and surrounding muscle fibers (m), is clearly evident after HHCB exposure (**c**). This data is also confirmed by the quantification of the total fluorescent signal (**d**). In addition, qPCR (**e**) and Western blot analyses (**f**) demonstrate an increase in this pro-inflammatory cytokine after HHCB administration. In panels (**a**–**c**), red indicates *Hm*AIF-1 immunoreactivity, while blue indicates DAPI-stained nuclei. $p < 0.05$ is considered statistically significative (* $p < 0.05$, ** $p < 0.01$, *** $p < 0.001$). Bars in (**a**–**c**): 100 µm.

In untreated and solvent-treated animals (Figure 6a,b), weakly stained Type 1 mucus cells appeared localized near the external layer, presenting a round shape typical of non-activated secretory cells. Similarly, type 2 mucus cells, which stained more intensely, displayed a round shape indicative of an inactive condition. In HHCB-treated leeches (Figure 6c), although the number of type 1 mucus cells did not significantly increase, as also graphically shown (Figure 6d), these cells appeared smaller and slightly less swollen compared with controls. This reduction in the cell size could indicate mucus release

following secretory activity or the presence of newly differentiated cells. In contrast, both the tissue distribution and morphology of type 2 secretory cells markedly changed, with these cells appearing more elongated, a feature typical of cells extending toward the epithelial layer to release mucus into the surrounding environment.

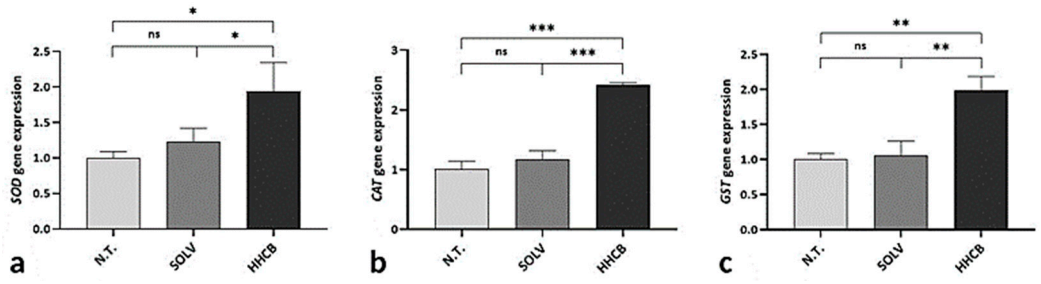

Figure 5. Evaluation of activation of leech antioxidant defensive mechanisms. The specific expression of antioxidant enzymes is evaluated by qPCR analyses. In detail, a significant increase in superoxide dismutase (*SOD*), glutathione S-transferase (*GST*), and catalase (*CAT*) genes is detectable in leeches treated with HHCB, compared to the controls (**a**–**c**). $p < 0.05$ is considered statistically significative (* $p < 0.05$, ** $p < 0.01$, *** $p < 0.001$).

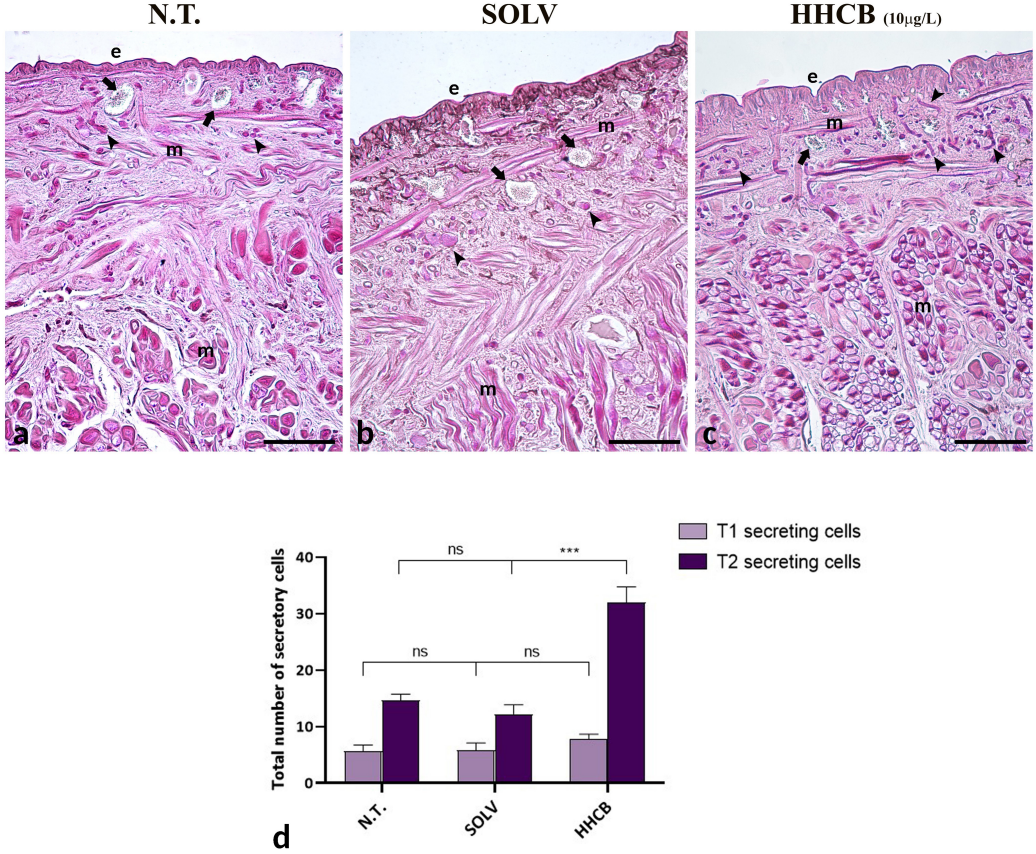

Figure 6. Organization of leech secretory cells. In both untreated (**a**) and solvent-treated (**b**) leeches, Type 1 (arrows) and Type 2 (arrowheads) mucus cells, located under the epithelium (e) and between the muscle fibers (m), are characterized by a rounded shape and inactive form. After HHCB exposure (**c**), despite the number of Type 1 cells (arrows) remaining unchanged, these cells appear reduced in terms of dimension. Instead, Type 2 mucus cells increase in number and appear more elongated (arrowheads), a morphology typical of activated secretory cells. The total count of both Type 1 and Type 2 mucus cells is represented in the graphs (**d**). $p < 0.05$ is considered statistically significative (*** $p < 0.001$). Bars in (**a**–**d**): 100 µm.

4. Discussion

The data collected in this preliminary study demonstrated that HHCB exposure triggers a marked inflammatory response in *H. verbana*, involving early angiogenic activation and an evident remodeling of the botryoidal tissue. Given that the formation of new blood vessels is a phenomenon closely associated with the initial inflammatory phases in these organisms [66], the activation of angiogenic processes was first assessed. In untreated leeches, tissues appear predominantly avascular, with only a few physiological vessels localized near the epithelium or between the underlying muscle fibers. Instead, a significant increase in their number is clearly visible after HHCB exposure. This evidence is also confirmed by the morphological evaluation of the botryoidal tissue, which is considered a multifunctional organ involved in angiogenesis, immune defense, and homeostasis regulation in leeches [67]. Notably, this tissue consists of two distinct cell populations: botryoidal cells and endothelial cells. Botryoidal cells are characterized by a large, rounded or oval morphology and contain numerous cytoplasmic granules of variable size. In contrast, endothelial cells are smaller and flatter, with a limited number of cytoplasmic granules. Interestingly, following injury, cytokine stimulation, or infection, the onset of vasculogenesis is associated with a marked remodeling of the botryoidal tissue. In particular, botryoidal cells undergo morphological changes, transitioning from compact elongated cords into pre-vascular tubular structures [68,69]. Thus, in control animals, it appears as a continuous cord of tightly packed cells, with epithelial and botryoidal cells closely associated and organized in compact strands. In contrast, HHCB drives the dissociation of these two cell types, leading to the consequent formation of a new vessel lumen. This condition is typically observed under stress stimulation or during the initial inflammatory response [66,70]. The activation of the angiogenic processes is also confirmed by the significant increase in both CD31 and VEGF-A expressions. The first is a specific endothelial receptor, well-known as a marker of these cells both in vertebrates [71] and in leeches [70]. VEGF-A is one of the main growth factors that promotes angiogenesis and endothelial cell proliferation [72]. In leeches, VEGF-like molecules have been described and are considered conserved mediators of vascular development, and their expression is typically associated with tissue remodeling, wound healing, and inflammation [73].

The formation of new blood vessels is also fundamental to promote the recruitment of innate immune cells, in particular macrophage-like cells, which are characterized by an intense phagocytic activity. These cells derive from hematopoietic stem precursors (HSPCs), produced in turn by the botryoidal tissue that, besides playing a crucial role in vasculogenesis, also possesses hematopoietic functions. Once activated, HSPCs exploited the formation of the new blood stream to reach the interested area and then differentiate into mature immune cells [70]. As already observed for other pollutants [74,75], HHCB induces a significant activation of macrophage-like cells, as confirmed by both optical and TEM analyses, as well as by the acid phosphatase (ACP) histoenzymatic assay. Interestingly, an increase in the ACP activity has been previously observed in these cells after pollutant exposure. Recent studies have demonstrated that some EMPs, such as PFAS and polyethylene terephthalate or polypropylene micro- and nanoplastics, are able to induce this condition [70,75]. Moreover, their activation is also confirmed by the high expression of *Hm*AIF-1, a fundamental pro-inflammatory marker normally expressed during the initial phase of inflammation. This calcium-binding protein is specifically produced by macrophage-like cells and plays a pivotal role in their recruitment, establishing a positive feedback mechanism [76,77].

The presence of HHCB not only causes a significant activation of the leech immune response, but also strongly promotes oxidative stress response. The significantly higher expression of specific antioxidant enzymes, such as superoxide dismutase (SOD), glutathione

S-transferase (GST), and catalase (CAT), is observable especially in HHCB-treated samples. The concomitant production of ROS and the upregulation of these enzymes are essential in these aquatic organisms to counteract the presence of possible foreign molecules [74,75,78]. Similar responses to pollutants have also been obtained in other invertebrates, in which the exposure to synthetic musk compounds such as HHCB has been associated with oxidative stress [45]. In detail, the alterations in antioxidant enzyme activity have been reported in several aquatic organisms exposed to HHCB, suggesting that oxidative stress represents a key mechanism underlying its biological effects [79]. Environmentally relevant concentrations of HHCB have been shown to induce oxidative damage accompanied by alterations in antioxidant biomarkers in the freshwater mussel *Dreissena polymorpha* [80]. Similarly, exposure experiments in the clam *Ruditapes philippinarum* reported changes in antioxidant enzyme activities, including superoxide dismutase (SOD) and catalase (CAT), indicating the activation of cellular defense mechanisms against ROS [81]. Comparable responses have also been described in primary producers such as freshwater algae, where HHCB exposure triggered oxidative stress pathways and metabolic perturbations associated with ROS accumulation [82]. In aquatic organisms, this imbalance between ROS generation and detoxification typically leads to the activation of antioxidant enzymes that play a pivotal role in maintaining cellular redox homeostasis.

Moreover, given that previous studies conducted in leeches revealed a close correlation between the expression of antioxidant enzymes and the activation of mucous cells [74], this aspect has also been assessed here. Specifically, in leeches, two distinct types of secretory cells are present: Type 1 mucous cells are located immediately below the epidermis and are easily recognizable by the lighter staining, while Type 2 cells are typically inner grouped [74,75]. As already observed also in several fish species, in which skin mucous cells are involved in the ROS production with the consequent alteration in the stress-related enzymes expression [83], also in *H. verbana* after HHCB administration, a variation in their number and morphology has been observed. In particular, although no significant variations were observed in Type 1 cells, except for changes in their size, which may reflect differences in secretory activity, Type 2 instead showed both numerical and morphological variations. Indeed, these cells exhibit an elongated shape, a feature typically associated with an activated state [74].

Although the present ecotoxicological study was limited to a single exposure concentration, the obtained results provide important preliminary evidence of the biological effects induced by HHCB and establish a valuable baseline for future investigations. Further studies involving multiple exposure concentrations, longer exposure times, and additional biological endpoints will be essential to better characterize dose–response relationships and to clarify the ecological relevance of synthetic musk contamination in aquatic environments.

5. Conclusions

Overall, the present findings contribute to a more comprehensive understanding of the toxicological effects of synthetic musk Galaxolide (HHCB) and highlight the urgent need for integrated environmental monitoring strategies that combine chemical analyses with in-depth biological and effect-based assessments. The results clearly demonstrate that HHCB cannot be considered biologically inert, as it is capable of disrupting organismal homeostasis through the activation of innate immune responses, as well as the induction of inflammatory and oxidative stress pathways.

Furthermore, this preliminary study conducted on a single concentration exposure confirms the medicinal leech as a valuable and sensitive model organism for ecotoxicological investigations. Indeed, these aquatic invertebrates exhibit complex immunological and metabolic responses within a well-characterized anatomical and functional framework,

making them particularly suitable as alternative bioindicator organisms for the detection of early sublethal effects induced by environmental contaminants.

Finally, the present study provides a useful baseline for future investigations aimed at better understanding the ecotoxicological impact of synthetic musks in non-conventional aquatic model organisms, including leeches, under different exposure scenarios and concentration ranges.

Author Contributions: A.R.: Formal analysis, Investigation, Writing—Review and Editing. G.M.: Formal analysis, Investigation, Writing—Review and Editing. M.B.: Validation, Writing—Review and Editing. L.P.: Validation, Data Curation, Investigation, Writing—Review and Editing. A.G.: Supervision, Funding Acquisition, Writing—Review and Editing. N.B.: Conceptualization, Project administration, Funding Acquisition, Validation; Writing—Original draft. S.T.: Conceptualization, Project administration, Funding Acquisition, Validation; Writing—Original draft. All authors have read and agreed to the published version of the manuscript.

Funding: This research was funded by FAR (Fondo di Ateneo per la Ricerca, University of Insubria) of A.G. and N.B.

Data Availability Statement: The data presented in this study are available on request from the corresponding author (please specify the reason for restriction, e.g., the data are not publicly available due to privacy or ethical restrictions).

Acknowledgments: Scientific support from the CRIETT Center of the University of Insubria (instrument code MIC01) is greatly acknowledged. G.M. is a PhD student of the course in Life Sciences and Biotechnology at the University of Insubria, Varese. The authors also thank Italian Leech Farm (ILFARM) Srl for providing leeches for the experimental work and Laura Marziali (CNR-IRSA) for initial support.

Conflicts of Interest: The authors declare no conflicts of interest.

Abbreviations

The following abbreviations are used in this manuscript:

ACP	Acid phosphatase
*Hm*AIF-1	Allograft inflammatory factor 1
BSA	Bovine serum albumin
CAT	Catalase
CD31	Cluster of differentiation 31
cDNA	Complementary DNA
DAPI	4′,6-diamidino-2-phenylindole
ECM	Extracellular matrix
EMPs	Emerging micropollutants
FITC	Fluorescein isothiocyanate
GST	Glutathione S-transferase
HHCB	Galaxolide (hexahydro-hexamethyl-cyclopenta[g]-2-benzopyran)
HSPCs	Hematopoietic stem precursor cells
NaCl	Sodium chloride
OCT	Optimal cutting temperature compound
PBS	Phosphate-buffered saline
PCR	Polymerase chain reaction
PFAS	Per- and polyfluoroalkyl substances
qPCR	Quantitative polymerase chain reaction
RIPA	Radioimmunoprecipitation assay buffer
RNA	Ribonucleic acid
ROS	Reactive oxygen species
SDS	Sodium dodecyl sulfate

SOD	Superoxide dismutase
TBS	Tris-buffered saline
TEM	Transmission electron microscopy
TRIS	Tris(hydroxymethyl)aminomethane
VEGF-A	Vascular endothelial growth factor A
WWTPs	Wastewater treatment plants

References

1. Petrie, B.; Barden, R.; Kasprzyk-Hordern, B. A Review on Emerging Contaminants in Wastewaters and the Environment: Current Knowledge, Understudied Areas and Recommendations for Future Monitoring. *Water Res.* **2015**, *72*, 3–27. [CrossRef] [PubMed]
2. Richardson, S.D.; Kimura, S.Y. Water Analysis: Emerging Contaminants and Current Issues. *Anal. Chem.* **2020**, *92*, 473–505. [CrossRef] [PubMed]
3. Zhao, X.; Wang, X.; He, J.; Feng, C.; Jin, X.; Leung, K.M.Y.; Xu, J.; Li, C.; Wang, J.; Liu, S.; et al. Time to Strengthen the Governance of New Contaminants in the Environment. *Nat. Commun.* **2025**, *16*, 7775. [CrossRef]
4. Deblonde, T.; Cossu-Leguille, C.; Hartemann, P. Emerging Pollutants in Wastewater: A Review of the Literature. *Int. J. Hyg. Environ. Health* **2011**, *214*, 442–448. [CrossRef] [PubMed]
5. Geissen, V.; Mol, H.; Klumpp, E.; Umlauf, G.; Nadal, M.; van der Ploeg, M.; van de Zee, S.E.A.T.M.; Ritsema, C.J. Emerging Pollutants in the Environment: A Challenge for Water Resource Management. *Int. Soil Water Conserv. Res.* **2015**, *3*, 57–65. [CrossRef]
6. Hollender, J.; van Bavel, B.; Dulio, V.; Farmen, E.; Furtmann, K.; Koschorreck, J.; Kunkel, U.; Krauss, M.; Munthe, J.; Schlabach, M.; et al. High Resolution Mass Spectrometry-Based Non-Target Screening Can Support Regulatory Environmental Monitoring and Chemicals Management. *Environ. Sci. Eur.* **2019**, *31*, 42. [CrossRef]
7. Escher, B.I.; Stapleton, H.M.; Schymanski, E.L. Tracking complex mixtures of chemicals in our changing environment. *Science* **2020**, *392*, 388–392. [CrossRef]
8. Yang, Y.; Ok, Y.S.; Kim, K.H.; Kwon, E.E.; Tsang, Y.F. Occurrences and Removal of Pharmaceuticals and Personal Care Products (PPCPs) in Drinking Water and Water/Sewage Treatment Plants: A Review. *Sci. Total Environ.* **2017**, *596–597*, 303–320. [CrossRef]
9. Gavrilescu, M.; Demnerová, K.; Aamand, J.; Agathos, S.; Fava, F. Emerging Pollutants in the Environment: Present and Future Challenges in Biomonitoring, Ecological Risks and Bioremediation. *New Biotechnol.* **2015**, *32*, 147–156. [CrossRef]
10. Vasilachi, I.C.; Asiminicesei, D.M.; Fertu, D.I.; Gavrilescu, M. Occurrence and Fate of Emerging Pollutants in Water Environment and Options for Their Removal. *Water* **2021**, *13*, 181. [CrossRef]
11. Arp, H.P.H.; Knutsen, H. Could We Spare a Moment of the Spotlight for Persistent, Water-Soluble Polymers? *Environ. Sci. Technol.* **2019**, *54*, 3–5. [CrossRef]
12. Santhappan, J.S.; Kalaiselvan, N.; Assis, S.M.; Amjith, L.R.; Glivin, G.; Mathimani, T. Origin, Types, and Contribution of Emerging Pollutants to Environmental Degradation and Their Remediation by Physical and Chemical Techniques. *Environ. Res.* **2024**, *257*, 119369. [CrossRef]
13. Bu, Q.; Ma, Y. Emerging Pollutants in the Environment: Occurrence, Fate, Risk Assessment and Degradation Methods. *Toxics* **2025**, *13*, 521. [CrossRef]
14. Sharma, T.; Singh, A.; Kumar, N.; Chauhan, G.; Singh, D.P.; Singh, A.; Rana, B.B. Emerging Pollutants in the Environment and Ecological Risks. In *Management and Mitigation of Emerging Pollutants*; Springer: Cham, Switzerland, 2023; pp. 1–20. [CrossRef]
15. Daughton, C.G.; Ternes, T.A. Pharmaceuticals and Personal Care Products in the Environment: Agents of Subtle Change? *Environ. Health Perspect.* **1999**, *107*, 907–938. [CrossRef]
16. Mitra, S.; Saran, R.K.; Srivastava, S.; Rensing, C. Pesticides in the Environment: Degradation Routes, Pesticide Transformation Products and Ecotoxicological Considerations. *Sci. Total Environ.* **2024**, *935*, 173026. [CrossRef] [PubMed]
17. Mishra, S.K.; Chowdhury, S.D.; Bhunia, P.; Sarkar, A.; Surampalli, R.Y.; Zhang, T.C. Degradation of Plastics and Formation of Primary and Secondary Microplastics. In *Microplastics in the Environment: Fate, Impacts, Removal, and Management*; Wiley: Hoboken, NJ, USA, 2025; pp. 43–68. [CrossRef]
18. Gewert, B.; Plassmann, M.M.; Macleod, M. Pathways for Degradation of Plastic Polymers Floating in the Marine Environment. *Environ. Sci. Process. Impacts* **2015**, *17*, 1513–1521. [CrossRef]
19. aus der Beek, T.; Weber, F.A.; Bergmann, A.; Hickmann, S.; Ebert, I.; Hein, A.; Küster, A. Pharmaceuticals in the Environment-Global Occurrences and Perspectives. *Environ. Toxicol. Chem.* **2016**, *35*, 823–835. [CrossRef] [PubMed]
20. Sun, J.; Dai, X.; Wang, Q.; van Loosdrecht, M.C.M.; Ni, B.J. Microplastics in Wastewater Treatment Plants: Detection, Occurrence and Removal. *Water Res.* **2019**, *152*, 21–37. [CrossRef]
21. Ngo, P.L.; Pramanik, B.K.; Shah, K.; Roychand, R. Pathway, Classification and Removal Efficiency of Microplastics in Wastewater Treatment Plants. *Environ. Pollut.* **2019**, *255*, 113326. [CrossRef] [PubMed]

22. Köck-Schulmeyer, M.; Villagrasa, M.; López de Alda, M.; Céspedes-Sánchez, R.; Ventura, F.; Barceló, D. Occurrence and Behavior of Pesticides in Wastewater Treatment Plants and Their Environmental Impact. *Sci. Total Environ.* **2013**, *458–460*, 466–476. [CrossRef]
23. Sutton, R.; Xie, Y.; Moran, K.D.; Teerlink, J. Occurrence and Sources of Pesticides to Urban Wastewater and the Environment. *ACS Symp. Ser.* **2019**, *1308*, 63–88. [CrossRef]
24. Lenka, S.P.; Kah, M.; Padhye, L.P. A Review of the Occurrence, Transformation, and Removal of Poly- and Perfluoroalkyl Substances (PFAS) in Wastewater Treatment Plants. *Water Res.* **2021**, *199*, 117187. [CrossRef]
25. Melitsiotis, A.; Christodoulis, K.; Karavasilis, M.; Bali, N.; Theodoropoulou, M.; Belay, M.H.; Davide, R.; Robotti, E.; Marengo, E.; Dondero, F.; et al. Remediation of Water from Per- and Poly-Fluoroalkyl Substances (Pfas) with Advanced Oxidation Processes: A Comparative Study of Ozonation and Photocatalysis. *Process Saf. Environ. Prot.* **2025**, *201*, 107477. [CrossRef]
26. Rotondo, D.; Gualandris, D.; Lorusso, C.; Braeuning, A.; Calisi, A.; Dondero, F. Impact of Short-Chain Perfluoropropylene Oxide Acids on Biochemical and Behavioural Parameters in Eisenia Fetida (Savigny, 1826). *J. Xenobiotics* **2025**, *15*, 2. [CrossRef] [PubMed]
27. Luo, Y.; Guo, W.; Ngo, H.H.; Nghiem, L.D.; Hai, F.I.; Zhang, J.; Liang, S.; Wang, X.C. A Review on the Occurrence of Micropollutants in the Aquatic Environment and Their Fate and Removal during Wastewater Treatment. *Sci. Total Environ.* **2014**, *473–474*, 619–641. [CrossRef]
28. Balci, E.; Genisoglu, M.; Sofuoglu, S.C.; Sofuoglu, A. Indoor Air Partitioning of Synthetic Musk Compounds: Gas, Particulate Matter, House Dust, and Window Film. *Sci. Total Environ.* **2020**, *729*, 138798. [CrossRef] [PubMed]
29. Srinivasulu, M.; Chandra, M.S.; Gooty, J.M.; Madhavi, A. Personal Care Products—Fragrances, Cosmetics, and Sunscreens—In the Environment. In *Environmental Micropollutants: A Volume in Advances in Pollution Research*; Elsevier: Amsterdam, The Netherlands, 2022; pp. 131–149. [CrossRef]
30. Patel, S.; Homaei, A.; Sharifian, S. Need of the Hour: To Raise Awareness on Vicious Fragrances and Synthetic Musks. *Environ. Dev. Sustain.* **2020**, *23*, 4764–4781. [CrossRef]
31. Babayan, B.; Yesayan, T.; Melkumyan, M.; Mikaelyan, G.; Bagdasaryan, S.; Elbakyan, S.; Avanesyan, A.; Yesayan, A.; Sevoyan, G. Artificial Fragrances and Semisynthetic Perfumes: The Hidden Health Risks. *Funct. Food Sci.* **2025**, *5*, 621–632. [CrossRef]
32. Lange, C.; Kuch, B.; Metzger, J.W. Occurrence and Fate of Synthetic Musk Fragrances in a Small German River. *J. Hazard. Mater.* **2015**, *282*, 34–40. [CrossRef]
33. Li, J.; Lu, Y.; Chen, H.; Zheng, D.; Yang, Q.; Campos, L.C. Synthetic Musks in the Natural Environment: Sources, Occurrence, Concentration, and Fate-A Review of Recent Developments (2010–2023). *Sci. Total Environ.* **2024**, *922*, 171344. [CrossRef]
34. Focardi, S.; Della Torre, C.; Monti, M.; Biagini, T.; Corsi, I. Synthetic Musks Fragrances in the Aquatic Environment: In Vitro Toxicological Studies of Their Biotransformation and Potential Negative Effects. *WIT Trans. Biomed. Health* **2011**, *15*, 183–194. [CrossRef]
35. Guerra-Martín, I.; Lodoso-Ruiz, E.; Trujillo-Rodríguez, M.J.; Ayala, J.H.; Pino, V. Occurrence of Fragrances in the Marine Environment. *Handb. Environ. Chem.* **2024**, *128*, 161–189. [CrossRef]
36. Arruda, V.; Simões, M.; Gomes, I.B. Synthetic Musk Fragrances in Water Systems and Their Impact on Microbial Communities. *Water* **2022**, *14*, 692. [CrossRef]
37. Luckenbach, T.; Epel, D. Nitromusk and Polycyclic Musk Compounds as Long-Term Inhibitors of Cellular Xenobiotic Defense Systems Mediated by Multidrug Transporters. *Environ. Health Perspect.* **2005**, *113*, 17–24. [CrossRef] [PubMed]
38. Nendza, M.; Kosfeld, V.; Schlechtriem, C. Consolidated Octanol/Water Partition Coefficients: Combining Multiple Estimates from Different Methods to Reduce Uncertainties in Log KOW. *Environ. Sci. Eur.* **2025**, *37*, 44. [CrossRef]
39. Petrarca, M.H.; Fernandes, J.O.; Cunha, S.C. Synthetic Musk Fragrances in Seafood: Occurrence, Influence of Culinary Practices, and In Vitro Bioaccessibility. *Handb. Environ. Chem.* **2024**, *128*, 265–291. [CrossRef]
40. Bonato, M.; Corrà, F.; Bellio, M.; Guidolin, L.; Tallandini, L.; Irato, P.; Santovito, G. PFAS Environmental Pollution and Antioxidant Responses: An Overview of the Impact on Human Field. *Int. J. Environ. Res. Public Health* **2020**, *17*, 8020. [CrossRef] [PubMed]
41. Metcalfe, C.D. Toxic Effects of Fragrances to Aquatic Organisms. *Handb. Environ. Chem.* **2024**, *128*, 37–46. [CrossRef]
42. Kim, S.; Ji, K. Effects of Synthetic Musk (AHTN, MK) on Zebrafish Development and Ecological Risk Assessment in Freshwater Environments. *J. Environ. Health Sci.* **2025**, *51*, 295–303. [CrossRef]
43. Tumová, J.; Šauer, P.; Golovko, O.; Koba Ucun, O.; Grabic, R.; Máchová, J.; Kocour Kroupová, H. Effect of Polycyclic Musk Compounds on Aquatic Organisms: A Critical Literature Review Supplemented by Own Data. *Sci. Total Environ.* **2019**, *651*, 2235–2246. [CrossRef] [PubMed]
44. Zhang, X.; Xu, Q.; Man, S.; Zeng, X.; Yu, Y.; Pang, Y.; Sheng, G.; Fu, J. Tissue Concentrations, Bioaccumulation, and Biomagnification of Synthetic Musks in Freshwater Fish from Taihu Lake, China. *Environ. Sci. Pollut. Res.* **2013**, *20*, 311–322. [CrossRef]
45. Ehiguese, F.O.; González-Delgado, M.J.; Garrido-Perez, C.; Araújo, C.V.M.; Martin-Diaz, M.L. Effects and Risk Assessment of the Polycyclic Musk Compounds Galaxolide® and Tonalide® on Marine Microalgae, Invertebrates, and Fish. *Processes* **2021**, *9*, 371. [CrossRef]

46. Liu, C.; Zhu, X.; You, L.; Gin, K.Y.H.; Chen, H.; Chen, B. Per/Polyfluoroalkyl Substances Modulate Plasmid Transfer of Antibiotic Resistance Genes: A Balance Between Oxidative Stress and Energy Support. *Water Res.* **2023**, *240*, 120086. [CrossRef] [PubMed]
47. Gatermann, R.; Biselli, S.; Hühnerfuss, H.; Rimkus, G.G.; Hecker, M.; Karbe, L. Synthetic Musks in the Environment. Part 1: Species-Dependent Bioaccumulation of Polycyclic and Nitro Musk Fragrances in Freshwater Fish and Mussels. *Arch. Environ. Contam. Toxicol.* **2002**, *42*, 437–446. [CrossRef] [PubMed]
48. Zhang, X.; Jing, Y.; Ma, L.; Zhou, J.; Fang, X.; Zhang, X.; Yu, Y. Occurrence and Transport of Synthetic Musks in Paired Maternal Blood, Umbilical Cord Blood, and Breast Milk. *Int. J. Hyg. Environ. Health* **2015**, *218*, 99–106. [CrossRef]
49. Arbulu, M.; Sampedro, M.C.; Unceta, N.; Gómez-Caballero, A.; Goicolea, M.A.; Barrio, R.J. A Retention Time Locked Gas Chromatography-Mass Spectrometry Method Based on Stir-Bar Sorptive Extraction and Thermal Desorption for Automated Determination of Synthetic Musk Fragrances in Natural and Wastewaters. *J. Chromatogr. A* **2011**, *1218*, 3048–3055. [CrossRef]
50. Fan, B.; Wang, X.; Li, J.; Gao, X.; Li, W.; Huang, Y.; Liu, Z. Deriving Aquatic Life Criteria for Galaxolide (HHCB) and Ecological Risk Assessment. *Sci. Total Environ.* **2019**, *681*, 488–496. [CrossRef]
51. Hu, Z.; Shi, Y.; Cai, Y. Concentrations, Distribution, and Bioaccumulation of Synthetic Musks in the Haihe River of China. *Chemosphere* **2011**, *84*, 1630–1635. [CrossRef]
52. Reiner, J.L.; Kannan, K. Polycyclic Musks in Water, Sediment, and Fishes from the Upper Hudson River, New York, USA. *Water Air Soil Pollut.* **2011**, *214*, 335–342. [CrossRef]
53. Zeng, X.; Hu, Q.; He, L.; Liu, Z.; Gao, S.; Yu, Z. Occurrence, Distribution and Ecological Risks of Organophosphate Esters and Synthetic Musks in Sediments from the Hun River. *Ecotoxicol. Environ. Saf.* **2018**, *160*, 178–183. [CrossRef]
54. Minier, C.; Pariselli, F.; Baltora-Rosset, S.; Billault, I.; Calvayrac, C.; Corbel, G.; Daniellou, R.; Denayer, F.-O.; Geoffroy, L.; Habert, R.; et al. Avis de l'Anses Relatif à l'évaluation Des Substances Inscrites Au Programme de Travail 2022–2023 de l'Agence Dans Le Cadre de l'évaluation Des Substances Sous REACH: 1,3,4,6,7,8-Hexahydro-4,6,6,7,8,8-Hexamethylindeno[5,6-c]Pyran (N° CE 214-946-9; N° CCAS 1222-05-5). In Proceedings of the Focus on Microscopy, Genoa, Italy, 24–27 March 2024; 14p. [CrossRef]
55. Tasselli, S.; Rogora, M.; Orrù, A.; Guzzella, L. Behaviour of Synthetic Musk Fragrances in Freshwaters: Occurrence, Relations with Environmental Parameters, and Preliminary Risk Assessment. *Environ. Sci. Pollut. Res.* **2023**, *30*, 109643–109658. [CrossRef]
56. Ferrario, C.; Finizio, A.; Villa, S. Legacy and Emerging Contaminants in Meltwater of Three Alpine Glaciers. *Sci. Total Environ.* **2017**, *574*, 350–357. [CrossRef]
57. Ding, T.; Li, W.; Cai, M.; Jia, X.; Yang, M.; Yang, B.; Li, J. Algal Toxicity, Accumulation and Metabolic Pathways of Galaxolide. *J. Hazard. Mater.* **2020**, *384*, 121360. [CrossRef]
58. Peck, A.M.; Hornbuckle, K.C. Synthetic Musk Fragrances in Lake Michigan. *Environ. Sci. Technol.* **2004**, *38*, 367–372. [CrossRef] [PubMed]
59. Otludil, B.; Otludil, B. Single and Combined Impact of Environmental Concentrations of Galaxolide (HHCB) and Tonalide (AHTN) on *Melanopsis praemorsa*: Evaluating Genotoxicity and Stress Response Mechanisms. *J. Appl. Toxicol.* **2026**, *46*, 384–400. [CrossRef] [PubMed]
60. Li, K.; Chen, C.; Wang, D.; Huang, H.; Yuan, Z.; You, J. Comparative Toxicity and Molecular Recognition of Galaxolide and Its Phototransformation Product Galaxolide Lactone in *Daphnia magna*. *Environ. Sci. Process. Impacts* **2026**. [CrossRef]
61. Ding, T.; Wei, L.; Yue, Z.; Lin, S.; Li, J. Individual and Combined Toxicity of Silver Nanoparticles and Triclosan or Galaxolide in the Freshwater Algae *Euglena* sp. *Sci. Total Environ.* **2023**, *887*, 164139. [CrossRef] [PubMed]
62. Petrauskienė, L. Water Toxicity Assessment Using Medicinal Leeches. *Aquat. Ecosyst. Health Manag.* **2001**, *4*, 203–208. [CrossRef]
63. Çelik, Z.; Aydın, H.; Ceylan, M. Acute Cadmium Toxicity in the Medicinal Leech *Hirudo verbana* Carena, 1820 with a Novel Biomarker for Aquatic Risk Assessment. *Ecotoxicology* **2025**, *35*, 3. [CrossRef]
64. Ben Ahmed, R.; Khaled, I.; El Ayari, T.; Saidi, I.; Harrath, A.H. Assessing the Effect of Polyethylene Microplastics in the Freshwater Leech *Erpobdella johanssoni* (Annelida, Hirudinida) Through Integrated Biomarkers and Histopathological Analysis. *Animals* **2025**, *15*, 1417. [CrossRef]
65. Tasselli, S.; Valenti, E.; Guzzella, L. Polycyclic Musk Fragrance (PMF) Removal, Adsorption and Biodegradation in a Conventional Activated Sludge Wastewater Treatment Plant in Northern Italy. *Environ. Sci. Pollut. Res.* **2021**, *28*, 38054–38064. [CrossRef] [PubMed]
66. Baranzini, N.; Pulze, L.; Acquati, F.; Grimaldi, A. Hirudo Verbana as an Alternative Model to Dissect the Relationship Between Innate Immunity and Regeneration. *Invertebr. Surviv. J.* **2020**, *17*, 90–98.
67. de Eguileor, M.; Grimaldi, A.; Tettamanti, G.; Congiu, T.; Protasoni, M.; Reguzzoni, M.; Valvassori, R.; Lanzavecchia, G. Ultrastructure and Functional Versatility of Hirudinean Botryoidal Tissue. *Tissue Cell* **2001**, *33*, 332–341. [CrossRef] [PubMed]
68. Grimaldi, A.; Tettamanti, G.; de Eguileor, M. Annelida: Hirudinea (Leeches): Heterogeneity in Leech Immune Responses. In *Advances in Comparative Immunology*; Springer: Cham, Switzerland, 2018; pp. 173–191. [CrossRef]
69. Grimaldi, A. Origin and Fate of Hematopoietic Stem Precursor Cells in the Leech *Hirudo medicinalis*. *Invertebr. Surviv. J.* **2016**, *13*, 257–268. [CrossRef]

70. Bon, C.; Pulze, L.; Amoroso, S.; Bertola, E.; Barbaro, M.; Tessaro, D.; Baranzini, N.; Grimaldi, A. Inflammatory and Oxidative Responses to PET Nanoplastics in the Leech Hirudo Verbana: A Comparative Analysis of Acute and Chronic Exposure. *Environ. Sci. Nano* **2025**, *13*, 427–446. [CrossRef]
71. Goncharov, N.V.; Popova, P.I.; Avdonin, P.P.; Kudryavtsev, I.V.; Serebryakova, M.K.; Korf, E.A.; Avdonin, P.V. Markers of Endothelial Cells in Normal and Pathological Conditions. *Biochem. (Mosc.) Suppl. Ser. A Membr. Cell Biol.* **2020**, *14*, 167–183. [CrossRef]
72. Matsumoto, K.; Ema, M. Roles of VEGF-A Signalling in Development, Regeneration, and Tumours. *J. Biochem.* **2014**, *156*, 1–10. [CrossRef]
73. Dvorak, H.F. Reconciling VEGF with VPF: The Importance of Increased Vascular Permeability for Stroma Formation in Tumors, Healing Wounds, and Chronic Inflammation. *Front. Cell Dev. Biol.* **2021**, *9*, 660609. [CrossRef]
74. Baranzini, N.; Pulze, L.; Bon, C.; Izzo, L.; Pragliola, S.; Venditto, V.; Grimaldi, A. Hirudo Verbana as a Freshwater Invertebrate Model to Assess the Effects of Polypropylene Micro and Nanoplastics Dispersion in Freshwater. *Fish Shellfish Immunol.* **2022**, *127*, 492–507. [CrossRef]
75. Calisi, A.; Baranzini, N.; Marcolli, G.; Bon, C.; Rotondo, D.; Gualandris, D.; Pulze, L.; Grimaldi, A.; Dondero, F. Evaluation of Per- and Polyfluoroalkyl Substances (PFAS) Toxic Effects on the Acute Inflammatory Response in the Medicinal Leech *Hirudo verbana*. *Chemosphere* **2024**, *366*, 143519. [CrossRef]
76. Baranzini, N.; Monti, L.; Vanotti, M.; Orlandi, V.T.; Bolognese, F.; Scaldaferri, D.; Girardello, R.; Tettamanti, G.; De Eguileor, M.; Vizioli, J.; et al. AIF-1 and RNASET2 Play Complementary Roles in the Innate Immune Response of Medicinal Leech. *J. Innate Immun.* **2019**, *11*, 150–167. [CrossRef]
77. Schorn, T.; Drago, F.; De Eguileor, M.; Valvassori, R.; Vizioli, J.; Tettamanti, G.; Grimaldi, A. The Allograft Inflammatory Factor-1 (AIF-1) Homologous in Hirudo Medicinalis (Medicinal Leech) Is Involved in Immune Response during Wound Healing and Graft Rejection Processes. *Invertebr. Surviv. J.* **2015**, *12*, 129–141.
78. Baranzini, N.; Calisi, A.; Marcolli, G.; Bon, C.; Rotondo, D.; Gualandris, D.; Pulze, L.; Grimaldi, A.; Dondero, F. Incomplete versus Sustained Innate-Immune Responses in the Medicinal Leech Following Chronic, Environmentally Relevant Per- and Polyfluoroalkyl Substance Exposure. *Environ. Health* **2025**. [CrossRef]
79. Aguirre-Martínez, G.V.; Buratti, S.; Fabbri, E.; DelValls, A.T.; Martín-Díaz, M.L. Potential of Environmental Concentrations of the Musks Galaxolide and Tonalide to Induce Oxidative Stress and Genotoxicity in the Marine Environment. *Mar. Environ. Res.* **2020**, *160*, 105019. [CrossRef]
80. Parolini, M.; Magni, S.; Traversi, I.; Villa, S.; Finizio, A.; Binelli, A. Environmentally Relevant Concentrations of Galaxolide (HHCB) and Tonalide (AHTN) Induced Oxidative and Genetic Damage in Dreissena Polymorpha. *J. Hazard. Mater.* **2015**, *285*, 1–10. [CrossRef]
81. Aguirre-Martínez, G.V.; Martín-Díaz, M.L. A Multibiomarker Approach to Assess Toxic Effects of Wastewater Treatment Plant Effluents and Activated Defence Mechanisms in Marine (*Ruditapes philippinarum*) and Fresh Water (*Corbicula fluminea*) Bivalve Species. *Ecotoxicology* **2020**, *29*, 941–958. [CrossRef]
82. Wang, J.; Wu, F.; Wang, X.; Ai, S.; Xi, J.; Liu, Z.; Wang, X. From Microbiota to Metabolism: Unveiling the Hidden Ecological Threat of Galaxolide (HHCB) to Zebrafish through Aquatic Microcosm. *Environ. Int.* **2025**, *202*, 109683. [CrossRef]
83. Espinosa-Ruíz, C.; Esteban, M.Á. Wound-Induced Changes in Antioxidant Enzyme Activities in Skin Mucus and in Gene Expression in the Skin of Gilthead Seabream (*Sparus aurata* L.). *Fishes* **2021**, *6*, 15. [CrossRef]

Disclaimer/Publisher's Note: The statements, opinions and data contained in all publications are solely those of the individual author(s) and contributor(s) and not of MDPI and/or the editor(s). MDPI and/or the editor(s) disclaim responsibility for any injury to people or property resulting from any ideas, methods, instructions or products referred to in the content.